Journal of Catalysis 284 (2011) 236–246

Contents lists available at SciVerse ScienceDirect

Journal of Catalysis

journal homepage: www.elsevier.com/locate/jcat

The role of chlorine and additives on the density and strength of Lewis and Brønsted acidic sites of γ-Al_2O_3 support used in oxychlorination catalysis: A FTIR study

N.B. Muddada [a], U. Olsbye [a], T. Fuglerud [b], S. Vidotto [c], A. Marsella [c], S. Bordiga [d], D. Gianolio [d], G. Leofanti [e], C. Lamberti [d,*]

[a] inGAP Centre of Research-based Innovation, Department of Chemistry, University of Oslo, Sem Saerlandsvei 26, N-0315 Oslo, Norway
[b] Technology and Projects, INEOS ChlorVinyls, Heroya Industrial Park, N-3936, Porsgrunn, Norway
[c] Vinyls R&D Team, INEOS Technologies, Via dell'Elettricità 39, I-30175, Venezia – Marghera, Italy
[d] Department of Inorganic, Physical and Materials Chemistry and NIS Centre of Excellence, and INSTM Reference Center, Università di Torino, Via P. Giuria 7, 10125 Torino, Italy
[e] Consultant, Via Firenze 43, 20010, Canegrate, Milano, Italy

ARTICLE INFO

Article history:
Available online 20 October 2011

Keywords:
$CuCl_2/Al_2O_3$
IR spectroscopy
Alumina
Lewis acidity
Brønsted acidity
CsCl dopant
$MgCl_2$ dopant
$LaCl_3$ dopant
Support modification
Ethylene oxychlorination catalyst

ABSTRACT

In two recent contributions [PCCP 12 (2010) 5605; Dalton Trans. 39 (2010) 8437], we combined *in situ* and in operando XANES/EXAFS, CO chemisorption and catalytic tests to elucidate the role that dopants (LiCl, KCl, CsCl, $MgCl_2$ $LaCl_3$) have in the nature, relative fraction, reducibility, and dispersion of Cu-phases on $CuCl_2/\gamma$-Al_2O_3 catalysts for C_2H_4 oxychlorination reaction, a key step of PVC chemistry. In the present work, we extend these studies by investigating the effect that the dopants have on the nature, population, and strength of surface Lewis and Brønsted sites of the support, using IR spectroscopy of adsorbed CO at liquid nitrogen temperature. The doping eliminates all the surface Lewis acidity in CsCl- and KCl-doped catalysts and strongly suppresses it in the remaining cases. The increase of the strength of the Brønsted sites is remarkable in all cases but the CsCl-doped one. To understand both the effect of Cl^- anions and dopant cations a set of dopant free, HCl-impregnated and of Cu-free dopant-impregnated supports have been investigated. Addition of chlorine decreases the density and the strength of Lewis sites, while it increases those of the Brønsted sites. Catalytic testing of each material revealed that formation of chlorinated by-products was directly correlated with the density of Lewis acid sites. Furthermore, an empirical correlation was found between the strength of the Brønsted acid sites of the support and the stretching frequency of CO adsorbed on the reduced fraction of the active copper chloride phase. The present study is aimed to complement the published literature on alumina, underlining the usefulness of the molecular approach made by IR spectroscopy low temperature adsorbed CO to investigate the surface of catalyst support.

© 2011 Elsevier Inc. All rights reserved.

1. Introduction

High surface area aluminas are widely used in catalysis as support for the active phase; this explains why they have been subjected to so large an investigation [1–18]. Among all applications, in this paper, we focus on the use of γ-Al_2O_3 as a support for $CuCl_2$ in the oxychlorination of ethylene [19–23], a key step in the PVC chemistry.

Nowadays, almost all the world production of PVC is obtained by the polymerization of vinyl chloride (VCM) [24], which is produced by cracking 1,2-dichloroethane (EDC) following reaction:

$$C_2H_4Cl_2 \rightarrow C_2H_3Cl + HCl \quad (1)$$

In its turn, EDC is produced by two parallel processes, direct chlorination (2) and oxychlorination (3) [24–26]:

$$C_2H_4 + Cl_2 \rightarrow C_2H_4Cl_2 \quad (2)$$

$$C_2H_4 + 2HCl + 1/2O_2 \rightarrow C_2H_4Cl_2 + H_2O \quad (3)$$

The latter reaction, recycling HCl produced by the cracking of 1,2-dichloroethane (1), is particularly important in industrial applications because it was specifically developed to reduce the Cl_2 consumption and the waste of HCl going outside the cycle, in agreement with the modern requirements of chemical industry [27–29].

The oxychlorination reaction (3) is performed at 490–530 K and 5–6 atm using both air and oxygen in fluid or fixed bed reactors. Commercial catalysts are produced by impregnation of γ-alumina

* Corresponding author at: Department of Inorganic, Physical and Materials Chemistry and NIS Centre of Excellence, Università di Torino, Via P. Giuria 7, 10125 Torino, Italy. Fax: +39 0116707855.
E-mail address: carlo.lamberti@unito.it (C. Lamberti).

0021-9517/$ - see front matter © 2011 Elsevier Inc. All rights reserved.
doi:10.1016/j.jcat.2011.08.014

with $CuCl_2$ (4–8 wt.% Cu). Other chlorides, (mainly alkaline or alkaline earth chlorides) in a variable concentration, are also added in order to improve the catalytic performances, making the catalyst more suitable for use in industrial reactors [27–31]. In particular, KCl is always present in the catalysts used in fixed bed technologies, sometimes together with other alkali-metal chlorides such as CsCl, NaCl or LiCl [32–34]. Rare-earth-metal chlorides such as $LaCl_3$, added to $CuCl_2$ and KCl, are also claimed in the patent literature [34]. $MgCl_2$ is the base additive in the catalysts used in fluid bed processes, where alkali-metal (such as LiCl) or rare-earth-metal chlorides (such as $LaCl_3$) can also be added [35–37]. Selection of the optimal catalyst for the heavy industrial process of ethylene oxychlorination is an important practical problem. The hydrogen chloride presence, high exothermicity of the reaction ($\Delta H = -239$ kJ/mol), and formation of volatile oxychlorides are all potential sources for modification of oxide supports and process kinetics, hence complicating the evaluation of mechanism of the primary and secondary reactions in oxychlorination. Due to the process scale, even a small decrease of selectivity results in significant consumption of feed and in production of undesired side-products, and thereby influences the economy of the entire PVC industry. So there is a great reason, why the oxychlorination catalyst is still under investigation and essential in PVC chemistry, despite being commercially established.

In spite of an abundant literature on the subject [19–22,27–31,38–44], a significant improvement of the knowledge of the system has been done only at the beginning of this century [19–22,44], even if limited to the base catalyst (containing only $CuCl_2$ without additives). It has been proved [19,20] that two different copper species are present on the catalyst dried at 500 K in N_2 flux: (i) a surface aluminate where the copper ions are hosted in the octahedral vacancies of γ-Al_2O_3 and (ii) a highly dispersed copper chloride. The former phase is formed at copper content lower than 0.95 wt.% Cu per 100 m^2 support, while the latter precipitates directly from the solution once the adsorptive capacity of alumina is exhausted.

Additionally, Lamberti et al. [23], performing an *in operando* time resolved XANES study, have determined the fraction of Cu(II) and Cu(I) of both $CuCl_2/\gamma$-Al_2O_3 and $KCl/CuCl_2/\gamma$-Al_2O_3 catalysts during the ethylene oxychlorination reaction in the 373–623 K range. It has been shown that the $KCl/CuCl_2/\gamma$-Al_2O_3 catalyst behaves differently from the base one, working in a prevailing oxidized state, while the $CuCl_2/\gamma$-Al_2O_3 catalyst works in the reduced state. Muddada et al. [45,46] have successively extended the study to several other additives using XANES, EXAFS, UV–Vis, IR of CO adsorbed at RT and catalytic tests in pulse reactor working in both depletive and pseudo steady state conditions.

In this paper, IR spectroscopy of adsorbed CO, at liquid nitrogen temperature, has been used to investigate the surface species present on the chlorine (via HCl)-doped samples and the $LiCl/CuCl_2/\gamma$-Al_2O_3, $KCl/CuCl_2/\gamma$-Al_2O_3, $CsCl/CuCl_2/\gamma$-Al_2O_3, $MgCl_2/CuCl_2/\gamma$-Al_2O_3, $CaCl_2/CuCl_2/\gamma$-Al_2O_3, $LaCl_3/CuCl_2/\gamma$-Al_2O_3, samples, representing the most used dopants present in the catalysts employed in both fixed and fluid bed technologies. The selectivity of the materials was investigated by catalytic tests under oxychlorination conditions.

The effect of additives on the $CuCl_2/\gamma$-Al_2O_3 system is extremely complex and can be summarized in the following five main points. (i) Additive cations may modify the engineering related to an improvement of the structural resistance of the catalysts pellets hosted inside the reactors, and to the decrease of the chemical and mechanic corrosion of the reactor walls, etc. (ii) Additives may have influence on the ability of $CuCl_2$ to be reduced by ethylene and of CuCl to be reoxidized by oxygen [23,45,46]. (iii) Additive cations may compete with Cu^{2+} cations in the saturation of cationic vacancies at the alumina surface, thus altering the fraction of Cu^{2+} cations present in the active phase [46], which has been established to be $CuCl_2$ for the bare $CuCl_2/\gamma$-Al_2O_3 in Refs. [19,20]. (iv) Additive cations can modify the Cu dispersion, favoring, or inhibiting the clustering of the particles of the active phase on the support [46]. (v) Additive cations modify the acidity of the support, which has been proved to be of both Lewis (surface Al^{3+} species) and Brønsted (surface Al–OH species) nature [21].

IR spectroscopy of adsorbed CO can answer only a small fraction of the question raised above: precisely, points (ii) and (v) for the reasons outlined below, while the remaining points have been addressed in our previous works [45,46]. CO interacts strongly with Cu^+ sites giving rise to stable $Cu^+\cdots CO$ adducts, characterized by an adsorption enthalpy in the 120 kJ $mol^{-1} < -\Delta H_{ads} < 80$ kJ mol^{-1} range [18,47–50], and by very high C–O extinction coefficients. Conversely, $Cu^{2+}\cdots CO$ adducts are much less stable and only very few IR studies have reported their formation.[51,52] Consequently, the intensity of the $Cu^+\cdots CO$ component is qualitatively correlated to the reducibility of the active Cu(II) phase; point (ii). CO molecule is ideal to probe surface Brønsted and Lewis sites and to evaluate how their strength and population is modified by the impregnation process needed to support both the active $CuCl_2$ and the dopant phases [1,53–55].

In this work, we systematically investigate the role of: (i) the activation temperature; (ii) the amount of chlorine added to the catalyst via $CuCl_2$, and/or dopant chloride or via HCl impregnation; (iii) the effect of the dopant chloride on the strength and population of surface Brønsted and Lewis acidic sites of γ-Al_2O_3, which are the main origin of undesired side products in ethylene oxychlorination catalysis [24,56–58]. Besides this specific target, our study has a much broader purpose, as the support can play an essential role for the catalytic activity of heterogeneous catalysts. As far as alumina is concerned, the ideal density of surface >Al–OH groups and the presence/absence of strong Al^{3+} Lewis sites are known to be two fundamental parameters in the performances of grafted active species, as demonstrated by several experimental and theoretical works [16,59–66]. Accordingly, the present study is aimed to complement the published literature on this hot topic in catalysis, showing how the molecular approach of using CO as probe to investigate the surface of the catalyst support can be highly informative. In particular, information are obtained on the species that, during the catalyst preparation steps, can be formed on the surfaces (>Al–Cl species) or can be covered and/or modified after impregnation (both Lewis and Brønsted sites) or can leave the surface after activation (–OH groups condensation and Cl^- release at higher temperatures).

2. Synthesis, experimental, and methods

All samples have been prepared by impregnation of a γ-alumina (Condea Puralox SCCa 30/170, surface area: 168 $m^2\ g^{-1}$, pore volume: 0.50 $cm^3\ g^{-1}$) with the aqueous solution of the corresponding chlorides following the incipient wetness method as described elsewhere [19]. After impregnation, the samples were dried at 393 K under a dry air flow for 1 h and then kept at room temperature (RT). To minimize aging effects [20], characterizations of samples have been performed 1 h after impregnation. Following the nomenclature already used in the previous papers [19–23,44–46,67,68], samples will be labeled according to wt.% content of the different metals (Cu and additive). As an example, sample Cu5.0 represents a 5.0 wt.% Cu loaded sample without additives, while sample K3.1Cu5.0 represents a catalyst prepared with 5.0 wt.% Cu plus 3.1 wt.% K impregnated in the chlorinated form (KCl). In all catalysts, the amount of copper has been fixed to 5 wt.%, while for the doped samples, an equal amount of additives atoms has been added, resulting in Li0.5Cu5.0, K3.1Cu5.0, Cs10.4Cu5.0, Mg1.9Cu5.0, Ca3.2Cu5.0, and La10.9Cu5.0 catalysts.

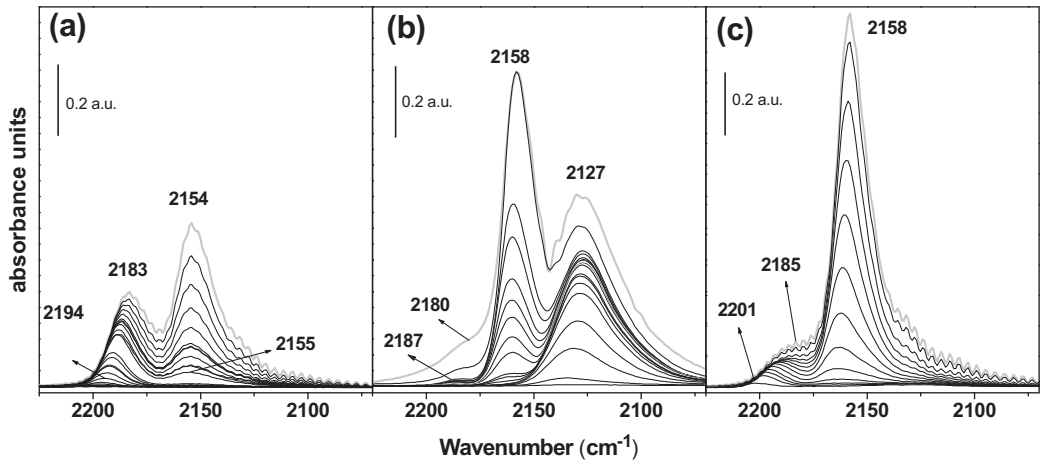

Fig. 1. IR spectra of CO adsorbed at liquid nitrogen temperature on: γ-Al_2O_3, Cu5.0; Cl2.8 samples, parts (a), (b), and (c) respectively. In all cases, before CO dosage samples where activated in dynamic vacuum at 503 K for 1 h. (a.u. = absorbance units). Figure composed using spectra from Ref. [21].

To investigate the effect of chlorine alone, two samples of chlorinated γ-alumina have been prepared by impregnating the γ-Al_2O_3 support with aqueous solution of HCl following the incipient wetness method with 1.4 and 2.8 Cl wt.% (hereafter Cl1.4 and Cl2.8), the higher concentration corresponding to the amount of Cl^- ions available for the Cu5.0 sample. The combined effect of dopant cations and Cl^- anions on the support has been investigated by preparing samples, again with the incipient wetness method on γ-alumina, with LiCl, KCl, CsCl, $MgCl_2$, $CaCl_2$, and $LaCl_3$ chlorides characterized by the same dopant atomic concentration used for the preparation of the catalysts (D^{n+}:Cu^{2+} = 1:1). Such samples will be labeled in the following as Li0.5, K3.1, Cs10.4, Mg1.9, Ca3.2, and La10.9, with obvious nomenclature.

For IR measurements, performed at liquid nitrogen temperature, a thin self-supporting wafer of the catalyst has been prepared and activated under dynamic vacuum at 503 K for 1 h inside an IR cell designed to allow *in situ* temperature treatments, reagents dosage and evacuation, and CO dosage. In these experiments, a CO

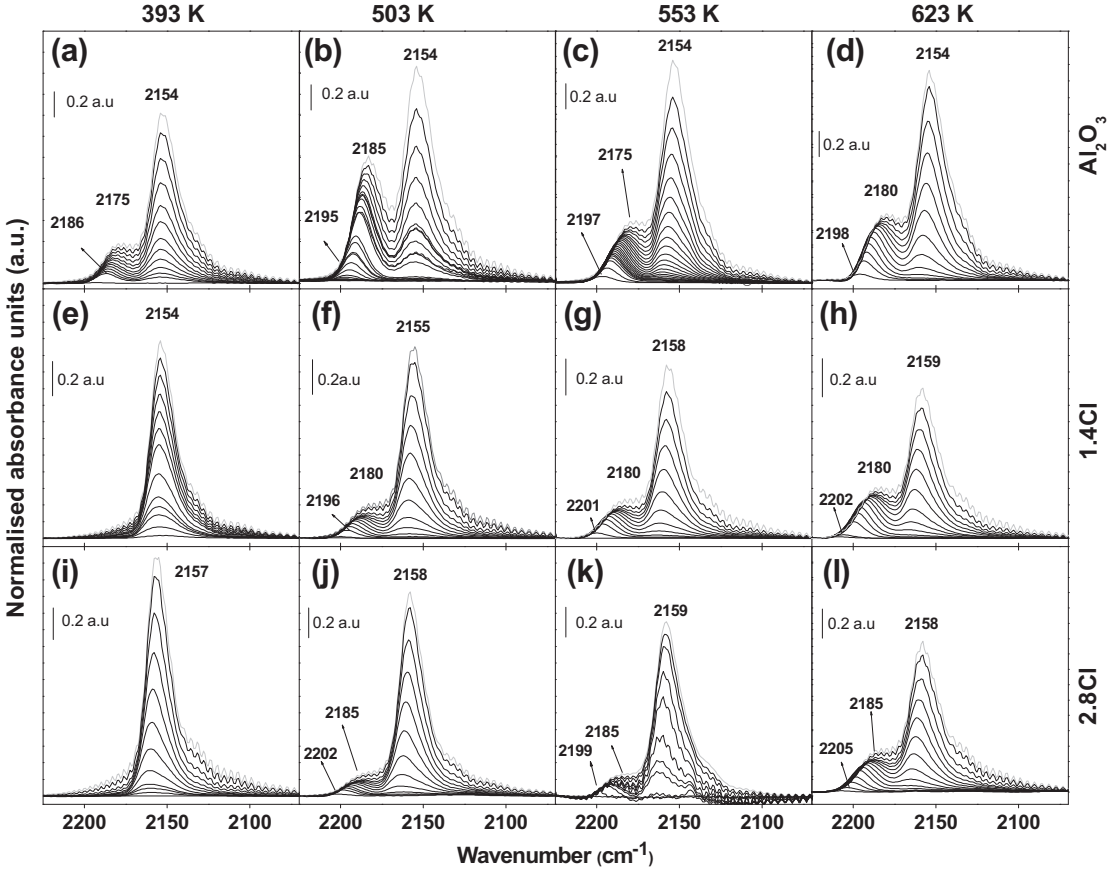

Fig. 2. IR spectra, in the C–O stretching region, of CO adsorbed at liquid nitrogen temperature on γ-Al_2O_3, parts (a–d), chlorinated γ-Al_2O_3, 1.4 Cl wt.% parts (e–h), and chlorinated γ-Al_2O_3, 2.8 Cl wt.% parts (i–l), activated in dynamic vacuum for 1 h at 393 (parts a, e, and i), 503 (parts b, f, and j), 553 (c, g, and k), and 623 K (parts d, h, and l) (a.u. = absorbance units). The spectra of the same experiments are reported in Fig. 3 in the O–H stretching region. Exact frequencies are reported in Table 1 for both low ($\theta \to 0$) and high ($\theta \to \theta_{max}$) coverage spectra.

equilibrium pressure of P_{CO} = 40 Torr (1 Torr = 133.3 Pa) is dosed, representing the maximum surface covering; successive expansions down to $P_{CO} = 10^{-3}$ Torr are then performed to investigate the lower coverages. This allows us to discriminate among species characterized by different adsorption enthalpies. The IR spectra have been recorded at 2 cm^{-1} resolution on a BRUKER FTIR 66 spectrometer equipped with a mercury cadmium telluride cryodetector. All spectra reported in this work are background subtracted, using the spectrum obtained before CO dosage as background. The intensity of the reported spectra has been normalized by the pellet weight.

Based on an experience longer than a decade [19–23,44,45,67,68], we know that IR spectroscopy on such systems suffers from reproducibility problems [46]. Indeed, the activation of the sample is very critical because both the surface dehydration and the fraction of reduced $CuCl_2$ phase strongly depend on the following factors: (i) temperature ramp; (ii) actual highest temperature reached (nominally 503 K in our experiments); (iii) the quality of the vacuum; (iv) the use of glass or metal (grease-free) vacuum lines, etc. Moreover, the exact $\tilde{\nu}(CO)$ values reported in the tables also depend on the exact minimum and maximum CO coverage reached that is defined by both the actual sample temperature (influenced by the contact between the sample pellet and the metallic part of the cell used for the heat transfer) and on the actual P_{CO}. This means that great care must be taken in performing these experiments in order to keep the experimental conditions adopted in all cases as close as possible. As an example, the two couples of experiments (Fig. 1a–Fig. 2b and Fig. 1c–Fig. 2j) should be ideally identical. They show, however, small differences (up to 2 cm^{-1}) in the observed components. The intensities cannot be compared because the spectra in Fig. 1 are reported in absolute absorbance units (pellets were not weighted) while those of Fig. 2 have been normalized by the pellet weight.

Catalytic testing was performed in a fixed bed quartz reactor with inner diameter of 10 mm. The reaction temperature was measured by a thermocouple in a quartz thermocouple well with outer diameter 3 mm, which was centered axially in the reactor. All feed lines were made of Teflon. In order to avoid temperature run-off, the ethene conversion was kept low, not exceeding 40% at 350 °C. The catalyst (200 mg, 250–450 μm) was diluted with graphite (400 mg, 250–450 μm). The feed gas composition was C_2H_4:HCl:O_2:He = 1:1.10:0.38:14.4 M ratio with total feed rate of 45 N ml/min. The effluent gas was analyzed by offline GC–MS (Agilent HP 5973 equipped with Gaspro column). GC–MS analysis was made after 60 min of isotherm at each temperature under reaction mixture. Reaction selectivity toward chlorinated by-products was estimated by dividing the sum of by-product areas by the EDC (ethylene dichloride) area at each temperature.

3. Results and discussion

CO is one of the most used probe molecule for the investigation of surface sites [1,3,12,18,50,69,70]. The interaction between CO and surface sites can be separated into an electrostatic, a covalent σ-dative, and a π-back donation contributions, the first two causing a blue shift of the $\tilde{\nu}(CO)$, while the last causes a red shift [18,49,71,72], with respect to the unperturbed molecule: $\tilde{\nu}_0(CO) = 2143\ cm^{-1}$. On the surface of a pure oxide CO probes both Brønsted and Lewis sites, so that on γ-Al_2O_3, we expect to observe $Al^{3+}\cdots CO$ adducts and, when the experiment is performed at liquid nitrogen temperature, also Al–OH···CO adducts [1,55]. In both cases, a blue shift $\Delta\tilde{\nu}(CO) = \tilde{\nu}(CO) - \tilde{\nu}_0(CO) > 0$ is expected, where usually the $\tilde{\nu}(CO)$ is in the 2230–2180 cm^{-1} and in 2155–2175 cm^{-1} ranges for $Al^{3+}\cdots CO$ and Al–OH···CO adducts, respectively. The $\tilde{\nu}(CO)$ value gives direct information on the acid strength of the site: higher is the $\Delta\tilde{\nu}(CO)$ stronger is the Lewis or Brønsted acidity of the probed site. Band intensity can provide information on the site abundance, once the corresponding extinction coefficient of the ν(CO) mode is properly evaluated. This occurs only very rarely and requires refined combination of IR and volumetric isotherms [73–75], so that usually only qualitative information on the surface abundances is obtained. In absence of such a sophisticated and complex approach, only semi-quantitative conclusions can be reached for carbonyl complexes formed on similar sites and resulting in similar positive $\Delta\tilde{\nu}(CO)$ values. It has indeed been empirically shown that the extinction coefficient of the ν(CO) mode has a smooth variation in the 2143–2230 cm^{-1} range, while it undergoes a rapid increase below 2143 cm^{-1} [3]. Consequently, band intensities are in first approximation proportional to the surface density of both Lewis and Brønsted sites, while no quantitative evaluation can be done for $Cu^+\cdots CO$ complexes (see below).

CO is an excellent probe molecule for Cu(I) sites [21,76–82], because of its strong interaction. From a measurement of the $\tilde{\nu}(CO)$ of a given Cu(I) carbonyl complex, information is obtained on the nature of the $Cu^+\cdots CO$ bond. On the contrary, the interaction of CO with Cu(II) is very week and has been only very rarely observed [51,52] In the present case, it is considered negligible.

3.1. Bare alumina, chlorinated alumina, and $CuCl_2$ supported alumina

The IR spectra of CO dosed on γ-Al_2O_3, Cu5.0 and Cl2.8 support, evacuated at 503 K, are reported in Fig. 1. Reported spectra were already discussed in Ref. [21]. In the case of the bare γ-Al_2O_3 (Fig. 1a), the two Lewis and Brønsted components discussed so far are well visible. At the lowest coverage, a single band, due to $Al^{3+}\cdots CO$ adducts, is observed at 2194 cm^{-1} that progressively shift downward to 2183 cm^{-1}. Once $Al^{3+}\cdots CO$ components reaches almost one half of its maximum intensity, a second component at 2154 cm^{-1}, which frequency is almost coverage independent, progressively rises up with increasing P_{CO}. This band is due to the formation of Al–OH···CO adducts. The observation of $Al^{3+}\cdots CO$ adducts on γ-Al_2O_3 supports activated at a so low temperature is unexpected, as usually, 503 K is not sufficient to remove OH groups from Al–OH species forming surface $>Al^{3+}$ Lewis sites with a coordinative vacancy.[1,53–55].

When the same experiment is performed on Cu5.0 catalyst heated at the same temperature (Fig. 1b), we observe that the component attributed to $Al^{3+}\cdots CO$ species is almost lost and that the Al–OH···CO adducts almost double in intensity and appears at a significantly higher frequency (compare the highest coverage spectra). It has already been proven that the modification in abundance and strength of the surface acidic sites on alumina is induced by the presence of chlorine [21], indeed a very similar effect can be obtained by exposing the oxide to HCl, see Fig. 1c.

Beside the evident modification on the surface acidity of the γ-Al_2O_3 support, a new band at 2134 cm^{-1} dominates the low coverage spectra of Cu5.0 sample (Fig. 1b) and progressively shifts downward to 2127 cm^{-1}. This band is the only component visible when the CO dosage is done at RT and is due to $Cu^+\cdots CO$ adducts formed on a very small fraction (1–2%) of copper reduced during the activation treatment [21,45,46,83,84]. Note that when the same experiment is performed on samples reduced by C_2H_4, this low frequency band is so intense that it fully saturates the IR spectrum [21,85]. This means that the intensity of the $Cu^+\cdots CO$ band on just activated samples does not reflect the amount of copper present on the sample (that will be 5 wt.% in all cases), but the reducibility of the $CuCl_2$ species [23,45,46].

The IR spectra reported in Fig. 1 clearly show that impregnating γ-Al_2O_3 with $CuCl_2$ not only forms the active phase for the oxychlorination reaction, but it has also important consequences on the properties of the support surface itself. It has previously been

demonstrated that the first fraction of supported Cu^{2+} reaching the surface is not recombining as $CuCl_2$ but saturates the octahedral surface vacancies of γ-alumina [19,46] and that the corresponding Cl^- anions are not lost but are anchored on the surface, forming >Al–Cl species [19] and modifying the abundance and the properties of acidic sites both Lewis and Brønsted nature. These modifications are of high relevance in the ethylene oxychlorination catalysis, as acid sites of alumina surface are the main origin of undesired side products [24,56–58].

Therefore, it is evident that it is important to go deeper into the effect that chlorination has on the surface of γ-Al_2O_3. As Cl^- species progressively leave the surface of alumina upon thermal treatments at increasing temperatures, it is important to monitor the available surface sites on bare and chlorinated alumina activated in the temperature range of interest for the ethylene oxychlorination reaction. The IR spectra of CO, dosed at liquid nitrogen temperature, on bare γ-Al_2O_3, and on chlorinated γ-Al_2O_3 (1.4 and 2.8 Cl wt.%), previously activated at increasing temperatures (393, 503, 553, and 623 K), are reported in Fig. 2 and in Fig. 3, for the C–O and O–H stretching region, respectively.

It has already been shown that the reaction of HCl with alumina induce the formation of >Al–Cl bonds because HCl is reacting with the surface >Al–O–Al< groups. Kitökivi et al. [85] in a well-documented NMR and IR study on the interaction of HCl, dosed from the gas phase, with bare alumina, found that two partially competitive reactions can take place, *i.e.*:

$$> Al{-}O{-}Al < + HCl \rightarrow > Al{-}OH + Cl{-}Al < \quad (4)$$

and

$$> Al{-}OH + HCl \rightarrow > Al{-}Cl + H_2O \quad (5)$$

The chlorination temperature and hydroxylation state of the alumina are the main factors driving the prevalence of one mechanism against the other. Eq. (5) prevails mostly with hydroxyl groups with low net negative charge on the surface, which easily undergo ion-exchange with Cl^- [85]. The amount of chlorine fixed by alumina depends on the temperature, and it is about 3 Cl^- anions/nm^2 at 373 K [85]. The value is substantially similar to that reported by Bailey and Wightman [86] at 313 K and by Tanaka and Ogosawara at 298 K [87].

Differently from Kitökivi et al., we chlorinated the surface from solution: this implies that a synergic action between H_2O and HCl occurs at the surface of alumina. Presence of water favors the opening of >Al–O–Al< bridges, increasing the number of surface >Al–OH groups according to:

$$> Al{-}O{-}Al < + H_2O \rightarrow > Al{-}OH + HO{-}Al < \quad (6)$$

Reaction (6) is progressively reversed upon thermal activation at increasing temperatures. The presence of chlorine on the surface, Eqs. (4) and (5), increases the acidic strength of remaining Brønsted sites, moving the $\tilde{\nu}$(C—O) in Al–OH···CO adducts from 2154 to 2158–2159 cm^{-1} thereby confirming the preliminary results reported in Ref. [21] and here summarized in Fig. 1.

The concepts discussed in the previous paragraphs are able to basically explain the whole set of spectroscopic data reported in

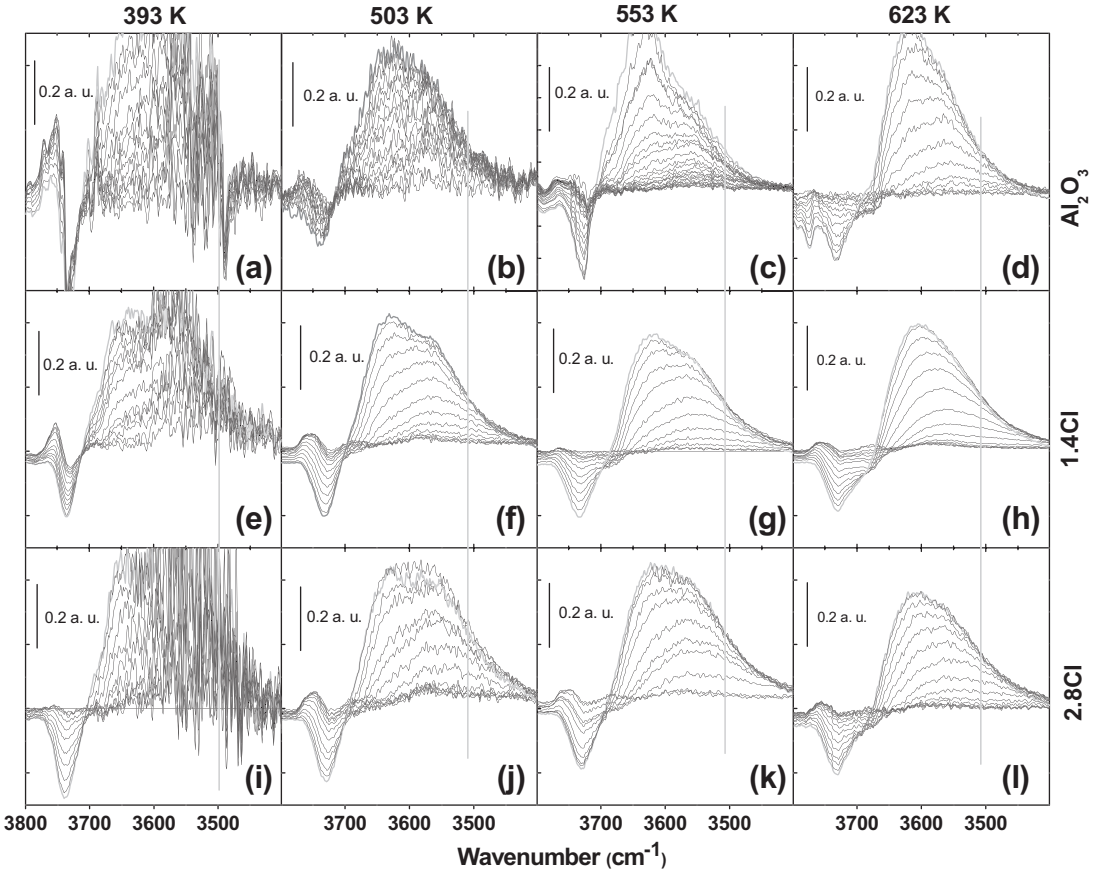

Fig. 3. Difference IR spectra, in the O–H stretching region, of CO adsorbed at liquid nitrogen temperature on γ-Al_2O_3, parts (a–d), chlorinated γ-Al_2O_3, 1.4 Cl wt.% parts (e–h), and chlorinated γ-Al_2O_3, 2.8 Cl wt.% parts (i–l), activated in dynamic vacuum for 1 h at 393 (parts a, e, and i), 503 (parts b, f, and j), 553 (c, g, and k), and 623 K (parts d, h, and l) (a.u. = absorbance units). The spectra of the same experiments are reported in Fig. 2 in the C–O stretching region. Due to the very high absorption in the O–H stretching region of high surface area γ-Al_2O_3, activated at relatively low temperatures, these spectra cannot be considered on a quantitative ground and only the evolution of the trends observed upon increasing the surface chlorination (top to bottom) or the activation temperature (left to right) can be qualitatively discussed.

Table 1
Summary of the CO stretching frequencies observed on the bare and chlorinated alumina supports at low ($\theta \to 0$) and high ($\theta \to \theta_{max}$) coverages for adducts formed on both Lewis (>Al^{3+}) and Brønsted (>Al–OH) sites. Data obtained from the spectra reported in Fig. 2.

Sample	Activation T (K)	$\bar{\nu}$(C—O) for adducts formed on Lewis sites		$\bar{\nu}$(C—O) for adducts formed on Brønsted sites	
		$\theta \to 0$ (cm^{-1})	$\theta \to \theta_{max}$ (cm^{-1})	$\theta \to 0$ (cm^{-1})	$\theta \to \theta_{max}$ (cm^{-1})
Al_2O_3	393	2186	~2175	2154	2154
Al_2O_3	503	2195	~2185	2155	2154
Al_2O_3	553	2197	~2175	2158	2154
Al_2O_3	623	2198	~2180	2158	2154
1.4Cl	393	Not observed	Not observed	2155	2154
1.4Cl	503	2196	~2180	2159	2155
1.4Cl	553	2201	~2180	2161	2158
1.4Cl	623	2202	~2180	2163	2159
2.8Cl	393	Not observed	Not observed	2160	2157
2.8Cl	503	2202	~2185	2163	2158
2.8Cl	553	2199	~2185	2163	2159
2.8Cl	623	2205	~2185	2162	2158

Fig. 2, Table 1, and Fig. 3. First, we observe that the density of surface hydroxyls of the samples activated at 393 K only (120 °C) is so high to results in spectra characterized by an almost complete absorption in the 3750–3500 cm^{-1} region, even if very thin pellets were prepared, (see the noisy spectra of the first column in Fig. 3). The increase of the activation temperature causes a progressive dehydroxylation of the surface according to the inverse of reaction (6) (Fig. 3 all rows from left to right). In the chlorinated aluminas, the dehydroxylation takes place also by reverse of reaction (4) with release of HCl. Note that chlorine leaving the surface at higher temperature (hot spots) is the main source for by-product formation. The progressive dehydroxylation upon heating is responsible for an increase of Lewis acid sites and of the parallel decrease of Brønsted ones.

High surface area hydrophilic materials like γ-Al_2O_3 activated at temperatures as low as 393 K (120 °C) still have the surface partially covered by molecularly adsorbed water molecules. This means that not all >Al–OH groups can be probed by CO molecules, as some of them are already engaged in H-bonded >Al–OH···OH_2 adducts. This explains the lower intensity of the band due to CO adsorbed on Brønsted sites in the sample Al_2O_3 activated at 393 K with respect to that of the sample activated at 503 K (first and second columns in Fig. 2).

For samples activated at 393 K, only (first column in Fig. 2) the addition of HCl cancels the vestiges of the Lewis sites, saturating the coordinative vacancies of >Al^{3+} sites with the formation of >Al–Cl species. For samples activated at 503 and 553 K, this effect does not involve the totality of the Lewis sites that are, however, strongly suppress (second and third column in Fig. 2). Finally, for the samples activated at higher temperature (623 K, last column in Fig. 2), the effect of HCl addition on the Lewis sites strength and population is almost negligible. The progressive lower effect of chlorination with increasing temperature is due to the removal of chlorine from the alumina surface by reverse of reaction (4). Note however that the influence on the increased acidity of the Brønsted sites still holds.

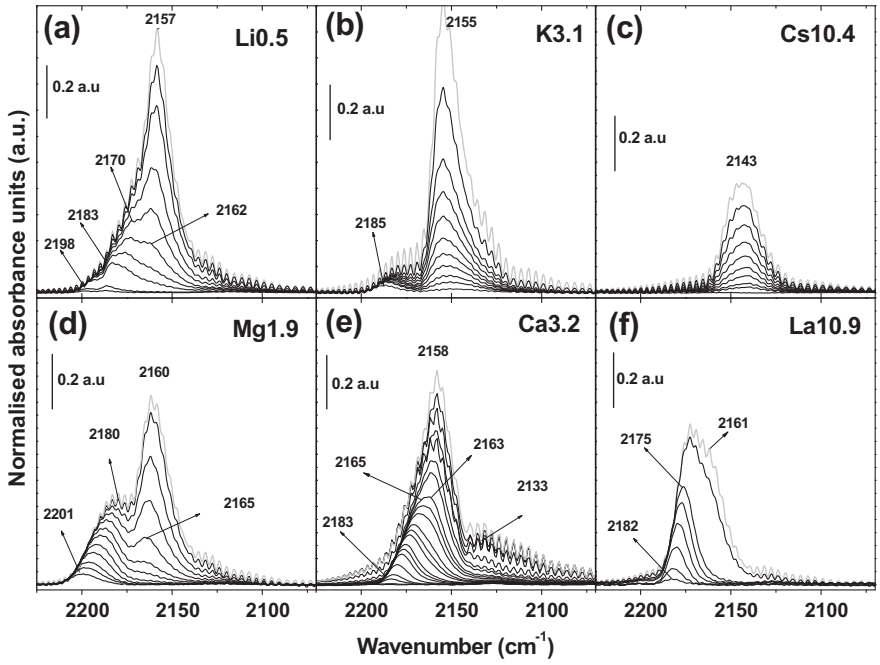

Fig. 4. IR spectra of CO adsorbed at liquid nitrogen temperature on: Li0.5, K3.1, Cs10.4, Mg1.9, Ca3.2, and La10.9, samples, parts (a–f), respectively. In all cases, before CO dosage samples where activated in dynamic vacuum at 503 K for 1 h. a.u. = absorbance units.

Table 2
Summary of the CO stretching frequencies observed on the doped alumina supports at low ($\theta \to 0$) and high ($\theta \to \theta_{max}$) coverages for adducts formed on both Lewis (>Al^{3+}) and Brønsted (>Al-OH) sites. Data obtained from the spectra reported in Fig. 4. For comparison also the data of the bare (Al_2O_3) and chlorinated (Cl1.4 and Cl2.8) supports and of the undoped catalyst (Cu5.0) are reported. All samples have been activated at 503 K. Li05, K3.1, and Cs10.4 samples carry the same amount of chlorine atoms as Cl1.4, corresponding to one half of that carried by Mg1.9, Ca3.2, and Cu5.0 and one third of that carried by La10.9.

Sample	$\tilde{\nu}$(C—O) for adducts formed on Lewis sites		$\tilde{\nu}$(C—O) for adducts formed on Brønsted sites	
	$\theta \to 0$ (cm^{-1})	$\theta \to \theta_{max}$ (cm^{-1})	$\theta \to 0$ (cm^{-1})	$\theta \to \theta_{max}$ (cm^{-1})
Li0.5	2198	~2170	2162	2157
K3.1	2185	~2180	2152	2155
Cs10.4	Not observed	Not observed	2141	2143
Mg1,9	2201	~2180	2165	2160
Ca3.2	2183	~2165	~2163	2158
La10.9	2182	~2175	~2165	~2161
Al_2O_3	2195	~2185	2155	2154
Cl1.4	2196	~2180	2159	2155
Cl2.8	2202	~2185	2163	2158
Cu5.0	2187	~2180	2160	2158

Table 3
Summary of CO stretching frequencies observed on alkali-, alkali-heart-, and La-halides as reported by literature.

Halide	$\tilde{\nu}$(CO) (cm^{-1})	Comments	Ref.
LiCl	2180, 2161, 2156	Three separated components	[91]
LiF	2155–2150	Progressive shift moving from $\theta \to 0$ to $\theta \to \theta_{max}$	[90]
LiF	2177, 2150	Two separated components	[91]
NaCl	2159–2156	Progressive shift moving from $\theta \to 0$ to $\theta \to \theta_{max}$	[90]
KCl	2153–2149	Progressive shift moving from $\theta \to 0$ to $\theta \to \theta_{max}$	[90]
NaI	2159–2157	Progressive shift moving from $\theta \to 0$ to $\theta \to \theta_{max}$	[90]
$MgCl_2$	2210, 2190, 2170	Three separated components[a]	[92]
$LaCl_3$	2184–2179; 2175–2166	Three separated components the first two shifting with θ	[93]
CuCl	2136–2134	Progressive shift moving from $\theta \to 0$ to $\theta \to \theta_{max}$	[77]

[a] Components at 2210, 2190, 2170 cm^{-1} have been attributed 3-, 4-, and 5-fold coordinated Mg^{2+} cations, respectively, according to the DFT calculations of Trubitsyn et al. [94].

3.2. Copper-free, dopant chloride supported on alumina

Coming to supported cations, Li^+, K^+, Cs^+, Mg^{2+}, Ca^2+, and La^{3+} (D^{n+} in general) behave differently from copper because the selected dopant cations have no *d* electrons contributing to the bond with CO. The $D^{n+}\cdots CO$ interaction is consequently expected to be rather weak and mainly of electrostatic nature [18,88]. The D^{n+} centers, either hosted in the octahedral vacancy of alumina [46], or at the surface of supported DCl_n chloride nanoparticles, behave as surface Lewis centers resulting in a blue shift of the ν(CO) when probed by carbon monoxide. The low temperature IR spectra of CO dosed on LiCl, KCl, CsCl, $MgCl_2$, $CaCl_2$, and $LaCl_3$ supported on γ-Al_2O_3, at the same atomic concentration as in the doped catalysts, are reported in Fig. 4a–f respectively, while the exact frequencies at low ($\theta \to 0$) and high ($\theta \to \theta_{max}$) coverages are reported in Table 2. All samples have been activated at 503 K prior to CO dosage, so the comparison of the doped supports has to be made with the spectra reported in the second column of Fig. 2. In particular, comparison with Fig. 2f has to be made for samples Li0.5, K3.1, and Cs10.4 and, while samples Mg1.9 and Ca3.2 should refer to Fig. 2j because of the same amount of chlorine atoms. Sample La10.9 has 3 and 3/2 times the amount of Cl than in samples Cl1.4 and Cl2.8, respectively. To better understand the nature of the bands reported in Fig. 4, literature data on IR experiments of CO dosed on different chlorides are summarized in Table 3.

The addition of KCl and CsCl can be straightforwardly commented. Any vestige of Lewis acidity is totally canceled by deposition of CsCl (Fig. 4c), while it is strongly depressed by deposition of KCl, where only a minor fraction of the less acidic Lewis sites of alumina survives: the $\theta \to 0$ $\tilde{\nu}$(C—O) moves from 2196 cm^{-1} (Fig. 2f) down to 2185 cm^{-1} (Fig. 4b). The strength of the Brønsted sites is also considerably diminished. On Cs10.4 sample $\tilde{\nu}$(C—O) is so low that it corresponds to the stretching frequency of the unperturbed molecule (2143 cm^{-1}). Moreover, this band is due to much more labile CO species as it rapidly disappears upon reducing P_{CO}, much faster than in the case of Al_2O_3, Cl1.4, and Cl2.8 samples (Fig. 2b, f, and j). This is testified by the component of the roto-vibrational contour of the CO in the gas phase [89] always present in the spectra reported in Fig. 4b and c even at the lowest coverages. This spectroscopic evidences testified that the >Al–$OH\cdots CO \rightleftharpoons$ >Al–OH+ CO_{gas} equilibrium is displaced toward the gas phase. The much lower strength of the Brønsted sites at the surface of the support is due to an increased strength of the O–H bond due to increased basicity of oxygen atoms in close contact with K^+ and Cs^+ cations that counteracts the opposite effect of the Cl^- ions, see Section 3.1. The possible co-presence of $K^+\cdots CO$ or $Cs^+\cdots CO$ contributions in the broad bands reported in Fig. 4b,c cannot be excluded: indeed CO adsorbed on KCl results in a band in the 2153–2149 cm^{-1} region [90], see Table 3.

Li0.5 (Fig. 4a) sample behaves in a markedly different way. In this case, a significant fraction of Lewis and Brønsted sites is still present. At the lowest coverages, a very weak band at 2198 cm^{-1} suggests the presence of a negligible amount of free Al^{3+} species. According to literature data [91], the more intense component moving from 2183 to 2170 cm^{-1} upon increasing θ is due to $Li^+\cdots CO$ adducts on LiCl. Brønsted sites result in a component in the 2162–2157 cm^{-1}, so exhibiting a similar acidity than in the chlorinated alumina, see Fig. 2f and Table 1. Among alkali-chlorides, LiCl is not so efficient as KCl and as CsCl in making chemically inactive the support.

According to the literature [92], the spectra reported in Fig. 4d testifies that CO interacts with Mg^{2+} cation of highly dispersed

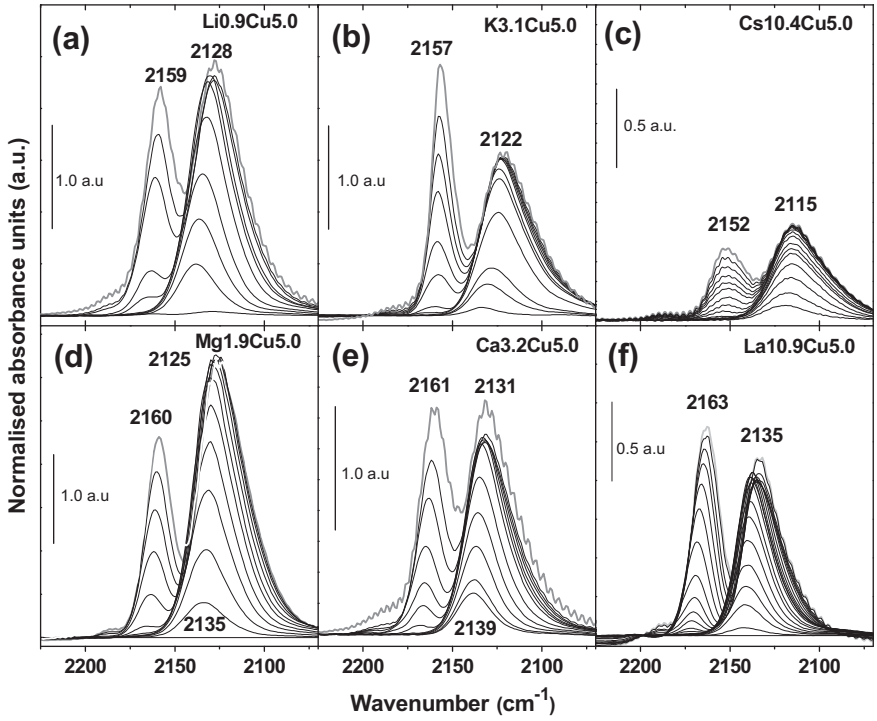

Fig. 5. IR spectra of CO adsorbed at liquid nitrogen temperature on: Li0.5Cu5.0, K3.1Cu5.0, Cs10.4Cu5.0, Mg1.9Cu5.0, Ca3.2Cu5.0, and La10.9Cu5.0, catalysts. . In all cases, before CO dosage samples where activated in dynamic vacuum at 503 K for 1 h. Please note that the ordinate scale is different, see the vertical marker (a.u. = absorbance units).

Table 4
Summary of the CO stretching frequencies observed on the doped catalysts at low ($\theta \to 0$) and high ($\theta \to \theta_{max}$) coverages for adducts formed on both Lewis (>Al^{3+}) and Brønsted (>Al–OH) sites. Data obtained from the spectra reported in Fig. 5. For comparison also the data of the bare (Al_2O_3) and chlorinated (Cl1.4 and Cl2.8) supports and of the undoped catalyst (Cu5.0) are reported. All samples were activated at 503 K. (s) = strong; (m) = medium; (w) = weak; (vw) = very weak.

Sample	$\bar{\nu}$(CO) for adducts formed on Lewis sites		$\bar{\nu}$(CO) for adducts formed on Brønsted sites		$\bar{\nu}$(CO) for adducts formed on Cu^+ sites	
	$\theta \to 0$ (cm^{-1})	$\theta \to \theta_{max}$ (cm^{-1})	$\theta \to 0$ (cm^{-1})	$\theta \to \theta_{max}$ (cm^{-1})	$\theta \to 0$ (cm^{-1})	$\theta \to \theta_{max}$ (cm^{-1})
Li0.5Cu5.0	2190 (vw)	~2180 (w)	2164	2159	2139	2128
K3.1Cu5.0	Not observed	Not observed	2159	2157	2132	2122
Cs10.4Cu5.0	Not observed	Not observed	2153	2152	2119	2115
Mg1.9Cu5.0	~2190 (wv)	~2185 (vw)	2165	2160	2135	2125
Ca3.2Cu5.0	~2200 (wv)	~2190 (vw)	2166	2161	2139	2131
La10.9Cu5.0	~2200 (wv)	~2190 (vw)	2170	2163	2139	2135
Al_2O_3	2195	~2185 (s)	2155	2154	–	–
Cl1.4	2196	~2180 (m)	2159	2155	–	–
Cl2.8	2202	~2185 (m)	2163	2158	–	–
Cu5.0	2187	~2180 (w)	2160	2158	2134	2127

$MgCl_2$, see Table 3. We cannot exclude that some >Al^{3+} species, not saturated by Cl^-, could contribute to the band in the 2201–2180 cm^{-1} range; however, this last one remains dominated by the $Mg^{2+}\cdots CO$ contributions. In this case, the acidity of Brønsted sites is further increased even with respect to the chlorinated alumina Fig. 2j, moving from 2165 to 2160 cm^{-1} upon coverage increase.

The spectra collected on La10.9 sample (Fig. 4f) are very close to those reported by the Weckhuysen group on thermally heated $LaCl_3{\cdot}7H_2O$ model compound [93]. This close correspondence (compare the frequencies reported in Tables 2 and 3) clearly shows that, on La10.9 sample, >Al^{3+} species are no more available, being the available Lewis sites La^{3+} cations of the highly dispersed $LaCl_3$ phase. Also in this case, the strength of the Brønsted sites (presumably at about 2161 cm^{-1}) is further increased with respect to the chlorinated alumina: it is difficult to discriminate whether this is due to La^{3+} or to the higher amount of chlorine atoms, equivalent to a chlorinated alumina by HCl at 4.2 wt.%.

The case of Ca3.2 sample is discussed at last because we were unable to find in the literature IR spectra of CO adsorbed at low temperature on highly dispersed $CaCl_2$. However, on the basis of the comparison with the other doped aluminas, we attribute the band moving from 2183 to 2165 cm^{-1} (Fig. 4e and Table 2) to $Ca^{2+}\cdots CO$ adducts formed on highly dispersed $CaCl_2$ particles. In this case, the strength of the Brønsted sites (2158 cm^{-1}) is comparable to that of the chlorinated alumina (Fig. 2j).

Summarizing, all dopants significantly reduce the fraction of available >Al^{3+} Lewis sites, mainly due to the formation of surface >Al–Cl species. This blocking effect of Lewis sites is important for limiting the by-product formation. In Li0.5, Mg1.9, Ca3.2, and La10.9 cases, this absence is replaced by a new acidity of Lewis nature due to appearance of D^{n+} surface sites. No Lewis sites, of whatever origin, are available to CO after impregnation with CsCl and very few and weak remain after KCl impregnation. With respect to chlorinated alumina (Section 3.1), the Brønsted acidity is completely (almost completely) quenched by CsCl (KCl) impregnation,

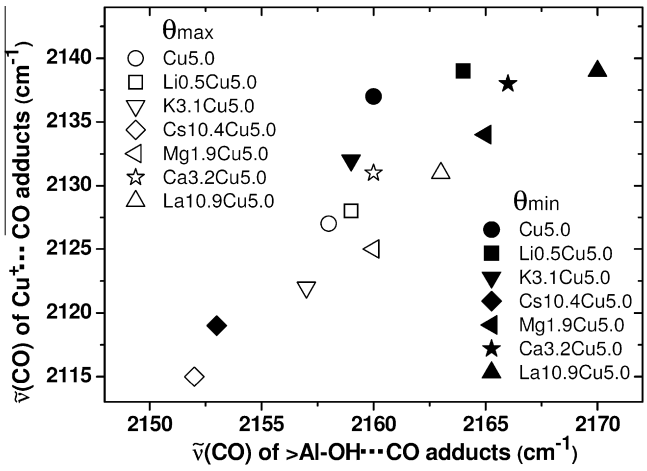

Fig. 6. Empirical correlation between the $\tilde{\nu}$(CO) of $Cu^{+}\cdots CO$ adducts and that of >Al–OH···CO adducts formed on Cu5.0 and on doped catalysts at low (full symbols) and high (open symbols) CO coverage θ. Data are taken from the IR spectra reported in Fig. 1a and in Fig. 5 (frequencies summarized in Table 4). Different symbols were used for different doped samples as reported in legend. The correlation between acid strength of surface Brønsted sites and frequency of CO adsorbed on the reduced fraction of the active phase is clearly demonstrated.

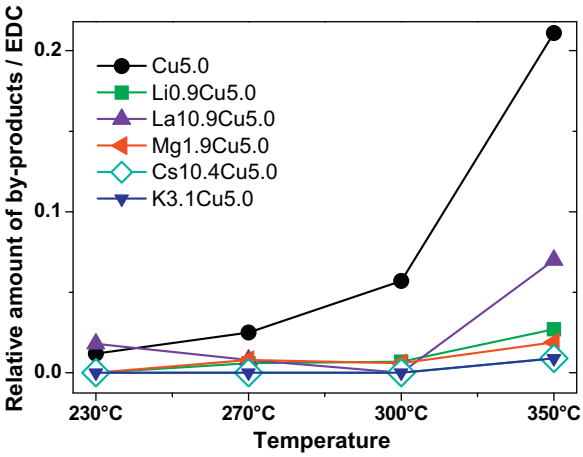

Fig. 7. Selectivity toward chlorinated by-products over the target product EDC (ethylene dichloride) for Cu5.0, Li0.5Cu5.0, K3.1Cu5.0, Cs10.4Cu5.0, Mg1.9Cu5.0, and La10.9Cu5.0 catalysts over the temperature range 230–350 °C. The reported data for each point is the ratio between relative amount of chlorinated by-products to relative amount of EDC. The selectivity toward chlorinated by-products follows in the order Cu5.0 > La10.9Cu5.0 > Li0.9Cu5.0 > Mg1.9Cu5.0 > K3.1Cu5.0 ≈ Cs10.4Cu5.0.

almost unchanged by LiCl and $CaCl_2$ doping and enhanced by $MgCl_2$ and $LaCl_3$ impregnation. Overall, these results indicate that the influence of the addition of alkali-metal cations, along with chlorine ion presence, is not only due to steric factor but also to probable electronic modifications. The modification of Lewis sites is more pronounced with increase of ionic radius of alkali metal, as evident in the case of Cs- and La-doped catalysts.

The here presented set of data complements the interesting work of de Miguel et al. [95], who investigated by IR spectroscopy of adsorbed CO Li- and K-doped γ-Al_2O_3 (194 m^2/g). In that case, precursors were $LiNO_3$ and KOH, requiring calcination of the samples at 773 K, so more strong Lewis sites were available with respect to the procedure adapted here. IR experiments were carried out at room temperature, so that only Lewis sites were monitored. Authors observed that addition of Li and K decreases the surface Lewis sites both in number and in strength, being larger the effect for K.

3.3. Doped $CuCl_2$ supported on alumina

The low temperature IR spectra of CO dosed on Li0.5Cu5.0, K3.1Cu5.0, Cs10.4Cu5.0, Mg1.9Cu5.0, Ca3.2Cu5.0, and La10.9Cu5.0 catalysts are reported in Fig. 5a–f respectively, while the exact frequencies at low ($\theta \to 0$) and high ($\theta \to \theta_{max}$) coverages are reported in Table 4. All samples were activated at 503 K prior to CO dosage, so a direct comparison can be done with: (i) the undoped catalyst (Fig. 1b); (ii) the spectra of the Cu-free doped supports (Fig. 4); and (iii) the chlorinated support (second column in Fig. 2).

The first overall impression is that the surface Lewis acidity is totally suppressed for CsCl- and KCl-doped catalysts, being strongly suppressed in the remaining cases. Comparing doped supports (Fig. 4) and doped catalysts (Fig. 5), the higher overall amount of chlorine deposited on the catalysts implies an increase of the Brønsted acidity in both $\tilde{\nu}$(CO) and adduct stability. When comparison is made on the bare support Fig. 1a, the increase of the strength of the Brønsted sites is remarkable in all cases but the CsCl-doped one (Fig. 5c), where significantly less acidic and less abundant Brønsted sites are observed.

This whole set of experimental data clearly demonstrate that the impregnation procedure with both the active $CuCl_2$ phase and the dopant phase have strong influence on the population, nature, and strength of both Lewis and Brønsted acid sites of the support, thus on the unwanted oxychlorination side products formation.

The lowest frequency band, due to $Cu^{+}\cdots CO$ adducts formed by the low fraction of Cu reduced during drying treatment under vacuum of the sample, falls in a wide range of frequency, depending on dopant cation. Compared to the band observed on undoped catalyst Cu5.0, the band of doped catalysts show the following sequence of increasing frequency: Cs10.4Cu5.0 < K3.1Cu5.0 < Li0.5Cu5.0 < -Cu5.0 < Mg1,9Cu5.0 < Ca3.2Cu5.0 < La10.9Cu5.0. This trends holds for both low and high CO coverages.

It is surprising to realize that in the set of spectra reported in Fig. 5, no clear evidence of the $D^{n+}\cdots CO$ adducts is present. Surface D^{n+} species may be partially covered by the supported $CuCl_2$ phase to be almost unreachable by CO. Besides the Cs case, note that the intensity of the bands due to $D^{n+}\cdots CO$ adducts at θ_{max} is between 0.05 and 0.4 a.u. (see Fig. 4), while maximum intensities of the IR bands reported in Fig. 5 lies in the 1.5–2.5 a.u. range. This means that if a fraction of the surface D^{n+} species is still available for CO after $CuCl_2$ impregnation, it may result in few $D^{n+}\cdots CO$ adducts giving rise to the unresolved high frequency tails of the IR bands reported in Fig. 5.

From the complete set of data, reported in Figs. 1b and 5, an empirical correlation between acid strength of surface Brønsted sites and frequency of CO adsorbed on the reduced fraction of the active phase is clearly demonstrated, as shown by the scattered symbols reported in Fig. 6. The greater is the strength of the surface Brønsted sites, the higher is the stretching frequency of the $Cu^{+}\cdots CO$ adducts formed on the fraction of reduced active phase. This proves a clear influence that the acidity of the support has on the electronic and coordinative states of the surface Cu^{+} sites of the active copper chloride phase.

3.4. Catalytic testing of by-product formation

The effect of dopant nature on catalyst selectivity is a main topic of this work. Fig. 7 shows the ratio of relative amount of chlorinated by-products (mainly ethyl chloride, but also including C_2H_3Cl, $C_2H_2Cl_2$, CCl_4, $C_2H_3Cl_3$) and target product EDC for each material in the 230–350 °C interval. It is clear that the undoped material (Cu5.0) produced the highest fraction of chlorinated

by-products, in spite of an intermediate conversion between K-, Cs-doped catalysts at the low activity side and Li-, Mg-, La-doped catalysts at the high activity side [45]. K3.1Cu5.0 and Cs10.4Cu5.0 catalysts, which had the lowest density of Lewis acid sites, gave least by-product formation, while Li0.5Cu5.0, Mg1.9Cu5.0, and La10.9Cu5.0 catalysts gave somewhat higher fraction of by-product formation. The selectivity toward chlorinated by-products correlated directly with the density of Lewis acid sites; these results are in agreement with the literature studies [96]. Interestingly, no correlation was found between by-product selectivity and Brønsted acid strength. In conclusion, this study has demonstrated the selective masking of sites active for by-product formation by dopant addition.

4. Conclusions

This work complements three recent contributions [45,46,97], where we understood the role that dopants (LiCl, KCl, CsCl, $MgCl_2$, and $LaCl_3$) have in the nature, relative fraction, reducibility, and dispersion of Cu-phases on $CuCl_2/\gamma$-Al_2O_3 catalysts for oxychlorination reaction. In the present work, we investigated the effect of the dopants on the nature, population, and strength of the surface Lewis and Brønsted sites of the support using low temperature IR spectroscopy of adsorbed CO. To understand both the effect of Cl^- anions and dopant cations, a set of dopant-free, HCl-impregnated and of Cu-free dopant-impregnated supports were studied.

The impregnation of alumina with HCl reduces the amount and the acidic strength of the Lewis sites, saturating the coordinative vacancies of >Al sites with the formation of >Al–Cl species. Chlorination of the surface results in an increase of the acidity of the Brønsted sites.

For the copper-free samples, all dopants significantly reduce the fraction of available $>Al^{3+}$ Lewis sites, mainly due to the formation of surface >Al–Cl species, resulting in a similar effect as that obtained with HCl. In Li0.5, Mg1.9, Ca3.2, and La10.9 cases, this absence is replaced by a new acidity of Lewis nature due to appearance of D^{n+} surface sites. No Lewis sites are available to CO after impregnation with CsCl, and very few and weak remain after KCl impregnation. With respect to chlorinated alumina (Section 3.1), the Brønsted acidity is completely (almost completely) quenched by CsCl (KCl) impregnation, almost unchanged by LiCl and $CaCl_2$ doping, and enhanced by $MgCl_2$ and $LaCl_3$ impregnation.

Comparing doped supports and doped catalysts, the higher overall amount of chlorine deposited on the catalysts implies an increase of the Brønsted acidity in both $\tilde{\nu}(CO)$ and adduct stability. When comparison is made with the bare support, the increase of the strength of the Brønsted sites is remarkable in all cases but the CsCl-doped one, where significantly less acidic and less abundant Brønsted sites are observed. Lewis acidic sites are strongly depressed in all doped catalysts. From the whole set of data, an empirical correlation between acid strength of surface Brønsted sites and frequency of CO adsorbed on the reduced fraction of the active phase is clearly demonstrated proving a significant influence of the support on the active phase.

Finally, catalytic tests performed in a fixed bed reactor indicates that the selectivity toward chlorinated by-products correlates directly with the density of Lewis acid sites, in the order Cu5.0 > La10.9Cu5.0 > Li0.9Cu5.0 > Mg1.9Cu5.0 > K3.1Cu5.0 ≈ Cs 10.4Cu5.0.

Acknowledgments

We are indebted to E. Groppo, S. Chavan, and G. Magnacca for the stimulating discussions and for their master role in teaching the practical basis of IR spectroscopy of adsorbed species. This study is part of inGAP Centre of Research-based Innovation, which receives financial support from the Norwegian Research Council under Contract No. 174893.

References

[1] C. Morterra, G. Magnacca, Catal. Today 27 (1996) 497.
[2] C. Barth, M. Reichling, Nature 414 (2001) 54.
[3] A. Zecchina, D. Scarano, S. Bordiga, G. Spoto, C. Lamberti, Adv. Catal. 46 (2001) 265.
[4] S.W. Wang, A.Y. Borisevich, S.N. Rashkeev, M.V. Glazoff, K. Sohlberg, S.J. Pennycook, S.T. Pantelides, Nat. Mater. 3 (2004) 143.
[5] M. Trueba, S.P. Trasatti, Eur. J. Inorg. Chem. (2005) 3393.
[6] G. Busca, Chem. Rev. 107 (2007) 5366.
[7] C. Marquez-Alvarez, N. Zilkova, J. Perez-Pariente, J. Cejka, Catal. Rev. – Sci. Eng. 50 (2008) 222.
[8] H.Z. Liu, T. Jiang, B.X. Han, S.G. Liang, Y.X. Zhou, Science 326 (2009) 1250.
[9] J.H. Kwak, J.Z. Hu, D. Mei, C.W. Yi, D.H. Kim, C.H.F. Peden, L.F. Allard, J. Szanyi, Science 325 (2009) 1670.
[10] R. Pellegrini, G. Leofanti, G. Agostini, E. Groppo, M. Rivallan, C. Lamberti, Langmuir 25 (2009) 6476.
[11] F. Thibault-Starzyk, E. Seguin, S. Thomas, M. Daturi, H. Arnolds, D.A. King, Science 324 (2009) 1048.
[12] A. Vimont, F. Thibault-Starzyk, M. Daturi, Chem. Soc. Rev. 39 (2010) 4928.
[13] A. Srinivasan, C. Depcik, Catal. Rev. – Sci. Eng. 52 (2010) 462.
[14] G. Agostini, E. Groppo, A. Piovano, R. Pellegrini, G. Leofanti, C. Lamberti, Langmuir 26 (2010) 11204.
[15] U. Diebold, S.C. Li, M. Schmid, Ann. Rev. Phys. Chem. 61 (2010) 129.
[16] P. Sautet, F. Delbecq, Chem. Rev. 110 (2010) 1788.
[17] J.M. Basset, C. Coperet, D. Soulivong, M. Taoufik, J.T. Cazat, Acc. Chem. Res. 43 (2010) 323.
[18] C. Lamberti, A. Zecchina, E. Groppo, S. Bordiga, Chem. Soc. Rev. 39 (2010) 4951.
[19] G. Leofanti, M. Padovan, M. Garilli, D. Carmello, A. Zecchina, G. Spoto, S. Bordiga, G.T. Palomino, C. Lamberti, J. Catal. 189 (2000) 91.
[20] G. Leofanti, M. Padovan, M. Garilli, D. Carmello, G.L. Marra, A. Zecchina, G. Spoto, S. Bordiga, C. Lamberti, J. Catal. 189 (2000) 105.
[21] G. Leofanti, A. Marsella, B. Cremaschi, M. Garilli, A. Zecchina, G. Spoto, S. Bordiga, P. Fisicaro, G. Berlier, C. Prestipino, G. Casali, C. Lamberti, J. Catal. 202 (2001) 279.
[22] G. Leofanti, A. Marsella, B. Cremaschi, M. Garilli, A. Zecchina, G. Spoto, S. Bordiga, P. Fisicaro, C. Prestipino, F. Villain, C. Lamberti, J. Catal. 205 (2002) 375.
[23] C. Lamberti, C. Prestipino, F. Bonino, L. Capello, S. Bordiga, G. Spoto, A. Zecchina, S.D. Moreno, B. Cremaschi, M. Garilli, A. Marsella, D. Carmello, S. Vidotto, G. Leofanti, Angew. Chem. Int. Edit. 41 (2002) 2341.
[24] C.E. Wilkes, C.A. Daniels, J.W. Summers, PVC Handbook, Hanser Gardner, Munich, 2005.
[25] J.A. Allen, A.J. Clark, Rev. Pure Appl. Chem. 21 (1971) 145.
[26] S. Wachi, Y. Asai, Ind. Eng. Chem. Res. 33 (1994) 259.
[27] J.S. Naworski, E.S. Evil, in: B.E. Leach (Ed.), Applied Industrial Catalysis, vol. 1, Academic Press, New York, 1983.
[28] M.N. Newmann, Encyclopedia of Polymer Science and Engineering, Wiley, New York, 1985.
[29] M. Garilli, P.L. Fatutto, F. Piga, La Chimica e l'Industria, Milan 80 (1998) 333.
[30] A. Arcoya, A. Cortes, X.L. Seoane, Can. J. Chem. Eng. 60 (1982) 55.
[31] W.D. Mross, Catal. Rev. Sci. Eng. 25 (1983) 591.
[32] P.R. Laurer, G. Krome, L. Cordemans, R. Seifert, E. Danz, Euro Patent 54674, 1981.
[33] K. Shiozaki, A. Onischi, Euro Patent 62320, 1982.
[34] I. Fatutto, D. Carmello, A. Marsella, Euro Patent 1053789, 2000.
[35] H. Derieth, R. Walter, G. Weidenbach, M. Strebbele, Euro Patent 255156, 1988.
[36] J.S. Eden, J.A. Cowfer, US Patent 4849393, 1989.
[37] D. Carmello, M. Grilli, P. Fatutto, L. Caccialupi, Euro Patent 1045731, 1999.
[38] A. Baiker, W.L. Holstein, J. Catal. 84 (1983) 178.
[39] K. Rollins, P.A. Sermon, J. Chem. Soc. Chem. Commun. (1986) 1171.
[40] E.M. Fortini, C.L. Garcia, D.E. Resasco, J. Catal. 99 (1986) 12.
[41] P.A. Sermon, K. Rollins, P.N. Reyes, S.A. Lawrence, M.A. Martin Luengo, M.J. Davies, J. Chem. Soc. Farad. Trans. 1 (83) (1987) 1347.
[42] P.S. Sai Prasad, P. Kanta Rao, J. Chem. Soc. Chem. Commun. (1987) 951.
[43] C.L. Garcia, D.E. Resasco, J. Catal. 122 (1990) 151.
[44] C. Prestipino, S. Bordiga, C. Lamberti, S. Vidotto, M. Garilli, B. Cremaschi, A. Marsella, G. Leofanti, P. Fisicaro, G. Spoto, A. Zecchina, J. Phys. Chem. B 107 (2003) 5022.
[45] N.B. Muddada, U. Olsbye, L. Caccialupi, F. Cavani, G. Leofanti, D. Gianolio, S. Bordiga, C. Lamberti, Phys. Chem. Chem. Phys. 12 (2010) 5605.
[46] N.B. Muddada, U. Olsbye, G. Leofanti, D. Gianolio, F. Bonino, S. Bordiga, T. Fuglerud, S. Vidotto, A. Marsella, C. Lamberti, Dalton Trans. 39 (2010) 8437.
[47] Y. Kuroda, H. Onishi, T. Mori, Y. Yoshikawa, R. Kumashiro, M. Nagao, H. Kobayashi, J. Phys. Chem. B 106 (2002) 8976.
[48] V. Bolis, S. Maggiorini, L. Meda, F. D'Acapito, G. Turnes Palomino, S. Bordiga, C. Lamberti, J. Chem. Phys. 113 (2000) 9248.
[49] V. Bolis, A. Barbaglia, S. Bordiga, C. Lamberti, A. Zecchina, J. Phys. Chem. B 108 (2004) 9970.
[50] C. Lamberti, E. Groppo, G. Spoto, S. Bordiga, A. Zecchina, Adv. Catal. 51 (2007) 1.
[51] K. Hadjiivanov, H. Knozinger, J. Catal. 191 (2000) 480.

[52] C. Prestipino, L. Regli, J.G. Vitillo, F. Bonino, A. Damin, C. Lamberti, A. Zecchina, P.L. Solari, K.O. Kongshaug, S. Bordiga, Chem. Mater. 18 (2006) 1337.
[53] L. Marchese, S. Bordiga, S. Coluccia, G. Martra, A. Zecchina, J. Chem. Soc. Faraday Trans. 89 (1993) 3483.
[54] C. Morterra, G. Magnacca, N. Delfavero, Langmuir 9 (1993) 642.
[55] E.N. Gribov, O. Zavorotynska, G. Agostini, J.G. Vitillo, G. Ricchiardi, G. Spoto, A. Zecchina, Phys. Chem. Chem. Phys. 12 (2010) 6474.
[56] E. Finocchio, N. Rossi, G. Busca, M. Padovan, G. Leofanti, B. Cremaschi, A. Marsella, D. Carmello, J. Catal. 179 (1998) 606.
[57] A. Marsella, D. Carmello, B. Finocchio, B. Cremaschi, G. Leofanti, M. Padovan, G. Busca, Stud. Surf. Sci. Catal. 130 (2000) 1823.
[58] D. Carmello, E. Finocchio, A. Marsella, B. Cremaschi, G. Leofanti, M. Padovan, G. Busca, J. Catal. 191 (2000) 354.
[59] M. Digne, P. Sautet, P. Raybaud, P. Euzen, H. Toulhoat, J. Catal. 226 (2004) 54.
[60] J. Joubert, F. Delbecq, P. Sautet, E. Le Roux, M. Taoufik, C. Thieuleux, F. Blanc, C. Coperet, J. Thivolle-Cazat, J.M. Basset, J. Am. Chem. Soc. 128 (2006) 9157.
[61] C. Coperet, Dalton Trans. (2007) 5498.
[62] A. Salameh, A. Baudouin, J.M. Basset, C. Coperet, Angew. Chem. Int. Edit. 47 (2008) 2117.
[63] M. Digne, P. Raybaud, P. Sautet, D. Guillaume, H. Toulhoat, J. Am. Chem. Soc. 130 (2008) 11030.
[64] R. Wischert, C. Coperet, F. Delbecq, P. Sautet, ChemCatChem 2 (2010) 812.
[65] C.H. Hu, C. Chizallet, C. Mager-Maury, M. Corral-Valero, P. Sautet, H. Toulhoat, P. Raybaud, J. Catal. 274 (2010) 99.
[66] R. Wischert, C. Coperet, F. Delbecq, P. Sautet, Angew. Chem. Int. Edit. 50 (2011) 3202.
[67] C. Lamberti, C. Prestipino, S. Bordiga, G. Berlier, G. Spoto, A. Zecchina, A. Laloni, F. La Manna, F. D'Anca, R. Felici, F. D'Acapito, P. Roy, Nucl. Instrum. Meth. B 200 (2003) 196.
[68] C. Lamberti, S. Bordiga, F. Bonino, C. Prestipino, G. Berlier, L. Capello, F. D'Acapito, F.X. Llabres i Xamena, A. Zecchina, Phys. Chem. Chem. Phys. 5 (2003) 4502.
[69] K.I. Hadjiivanov, G.N. Vayssilov, Adv. Catal. 47 (2002) 307.
[70] G. Spoto, E.N. Gribov, G. Ricchiardi, A. Damin, D. Scarano, S. Bordiga, C. Lamberti, A. Zecchina, Prog. Surf. Sci. 76 (2004) 71.
[71] S.H. Strauss, J. Chem. Soc. Dalton Trans. (2000) 1.
[72] A.J. Lupinetti, S.H. Strauss, G. Frenking, Prog. Inorg. Chem. 49 (2001) 1.
[73] V. Bolis, G. Magnacca, C. Morterra, Res. Chem. Intermed. 25 (1999) 25.
[74] C. Morterra, G. Cerrato, V. Bolis, C. Lamberti, L. Ferroni, L. Montanaro, J. Chem. Soc. Faraday Trans. 91 (1995) 113.
[75] V. Bolis, B. Fubini, E. Garrone, C. Morterra, P. Ugliengo, J. Chem. Soc. Faraday Trans. 88 (1992) 391.
[76] C. Lamberti, S. Bordiga, M. Salvalaggio, G. Spoto, A. Zecchina, F. Geobaldo, G. Vlaic, M. Bellatreccia, J. Phys. Chem. B 101 (1997) 344.
[77] D. Scarano, P. Galletto, C. Lamberti, R. DeFranceschi, A. Zecchina, Surf. Sci. 387 (1997) 236.
[78] A. Zecchina, S. Bordiga, M. Salvalaggio, G. Spoto, D. Scarano, C. Lamberti, J. Catal. 173 (1998) 540.
[79] D. Scarano, S. Bordiga, C. Lamberti, G. Spoto, G. Ricchiardi, A. Zecchina, C.O. Arean, Surf. Sci. 411 (1998) 272.
[80] A. Zecchina, S. Bordiga, G.T. Palomino, D. Scarano, C. Lamberti, M. Salvalaggio, J. Phys. Chem. B 103 (1999) 3833.
[81] C. Lamberti, G.T. Palomino, S. Bordiga, G. Berlier, F. D'Acapito, A. Zecchina, Angew. Chem. Int. Edit. 39 (2000) 2138.
[82] C. Prestipino, L. Capello, F. D'Acapito, C. Lamberti, Phys. Chem. Chem. Phys. 7 (2005) 1743.
[83] G. Turnes Palomino, P. Fisicaro, S. Bordiga, A. Zecchina, E. Giamello, C. Lamberti, J. Phys. Chem. B 104 (2000) 4064.
[84] F.X. Llabres i Xamena, P. Fisicaro, G. Berlier, A. Zecchina, G. Turnes Palomino, C. Prestipino, S. Bordiga, E. Giamello, C. Lamberti, J. Phys. Chem. B 107 (2003) 7036.
[85] A. Kytokivi, M. Lindblad, A. Root, J. Chem. Soc. Faraday Trans. 91 (1995) 941.
[86] R.R. Bailey, J.P. Wightman, J. Colloid Interface Sci. 70 (1979) 112.
[87] M. Tanaka, S. Ogasawara, J. Catal. 16 (1970) 157.
[88] C. Lamberti, S. Bordiga, F. Geobaldo, A. Zecchina, C.O. Arean, J. Chem. Phys. 103 (1995) 3158.
[89] S. Bordiga, D. Scarano, G. Spoto, A. Zecchina, C. Lamberti, C.O. Arean, Vib. Spectrosc. 5 (1993) 69.
[90] E. Escalona Platero, D. Scarano, G. Spoto, A. Zecchina, Faraday Discuss. Chem. Soc. 80 (1985) 183.
[91] A. Lubezky, Y. Kozirovski, M. Folman, J. Electron Spectrosc. Relat. Phenom. 95 (1998) 37.
[92] V.A. Zakharov, E.A. Paukshtis, T.B. Mikenas, A.M. Volodin, E.N. Vitus, A.G. Potapov, Macromol. Symp. 89 (1995) 55.
[93] O.V. Manoilova, S.G. Podkolzin, B. Tope, J. Lercher, E.E. Stangland, J.M. Goupil, B.M. Weckhuysen, J. Phys. Chem. B 108 (2004) 15770.
[94] D.A. Trubitsyn, V.A. Zakharov, I.I. Zakharov, J. Mol. Catal. A – Chem. 270 (2007) 164.
[95] S.R. de Miguel, O.A. Scelza, A.A. Castro, J. Soria, Top. Catal. 1 (1994) 87.
[96] L. Salinas III, T.E. Morris, A.D. Harley, US Patent 5202511, 1989.
[97] D. Gianolio, N.B. Muddada, U. Olsbye, C. Lamberti, Nucl. Instrum. Methods Phys. Research B (2011), doi:10.1016/j.nimb.2011.08.004.